International Journal of Trend in Scientific Research and Development (IJTSRD)
Volume 7 Issue 6, November-December 2023 Available Online: www.ijtsrd.com e-ISSN: 2456 – 6470

Analysis of Stress and Deflection of Spur Gear by Using New Analytical Method Based on Taguchi Method and Finite Element Analysis

Khin Khin Thant, Than Than Htike

Mechanical Engineering Department, Yangon Technology University,
Insein Township, The Republic of the Union of Myanmar

ABSTRACT

One of the most important measures of transmission performance is the gear tooth root stress (TRS). High root stress can directly damage the gear tooth and indirectly affect the life of the gear. This paper considered reducing the stresses in the base of the change in the gear profile. Accurate calculation of the maximum tooth root stress (TRS) and deflection is fundamental to the prediction and optimization of gears. The Finite Element Method (FEM) gives accurate results. But, the calculation requires a lot of resources and time. Moreover, the results obtained from the Lewis, the ISO, and the AGMA methods were useful. This paper approved the results of the new method as useful as other methods. Therefore, in the current results, a new analytical method based on mechanic theory is created using exact profile equations to calculate stress and deflection. Firstly, the load sharing ratio is considered using the Taguchi method. Finally, tooth root stress and deflection are calculated from this profile. The result of tooth root stress obtained from the new method is compared with the FEM method. The result of the new method is found the consistent with FEM method.

KEYWORDS: *deflection, load sharing ratio, spur gear, tooth root stress (TRS)*

How to cite this paper: Khin Khin Thant | Than Than Htike "Analysis of Stress and Deflection of Spur Gear by Using New Analytical Method Based on Taguchi Method and Finite Element Analysis" Published in International Journal of Trend in Scientific Research and Development (ijtsrd), ISSN: 2456-6470, Volume-7 | Issue-6, December 2023, pp.404-410, URL: www.ijtsrd.com/papers/ijtsrd60165.pdf

IJTSRD60165

Copyright © 2023 by author (s) and International Journal of Trend in Scientific Research and Development Journal. This is an Open Access article distributed under the terms of the Creative Commons Attribution License (CC BY 4.0) (http://creativecommons.org/licenses/by/4.0)

INTRODUCTION

Tooth root stress (TRS) is one of the foremost performance that indices in gear design and research, holds significant importance. A high tooth root stress can lead to direct gear damage or have an indirect impact on overall gear performance. Accurately and ripidly calculating tooth root stress and deformation serves as a fundamental basis for gear structure design. Currently, there are two primary calculation models in use: the FEM model and the analytical model.

The FEM model is a widely adopted approach for obtaining accurate and direct measurements of stress in the base of gear tooth and deflection. It calculates in quantifying the impact of various factors, such as different gear periods, shapes, and slope deviations, on TRS [1,2]. Furthermore, the FEM model allows for the analysis of TRS in gears that cannot be effectively assessed by other models, such as thin-rimmed spur gears with inclined webs. This model accounts for factors like centrifugal load [3] and web angle [4] effects at high speeds. Additionally, the FEM model is versatile in reducing TRS by optimizing gear parameters to obtain better mechanical properties [5]. It is also a valuable tool for evaluating the performance enhancement resulting from gear tooth profile modifications [6]. Furthermore, it can assess the impact of tooth profile variations, machining errors, and assembly errors on TRS using a three-dimensional FEM model [7]. High contact ratio gears present a specific challenge, as their load sharing and deformation between teeth significantly affect TRS. The FEM model excels. in calculating these parameters, a task often difficult to achieve with other models. As a result, the scope of research encompasses both uniform [8] and profile modifications [9] for high contact ratio gears, as well as their optimization to reduce TRS [10–12]. To improve computational efficiency, new numerical models have been developed [13].

This paper analyzed stress on the root of tooth and deflection

generated in a new method. In this article, the stresses on the base of the gear tooth and deflection values were compared with FEM result. The alternative combined effect of the pressure angles, the face width of gear, the addendum coefficients of variation, and the corner radii adjusted are determined in the new model design using the Taguchi method.

A. Gear Parameters and Material

The gears data are selected from the lathe machine and the mechanical properties of the gear material are shown in Table I and Table II. The gear tooth profile curve of the new method has used this parameter and material properties as the profile shape is shown in figure.1.

TABLE I. Geometric parameters in gear parameters

Parameters	Values
Number of teeth pinion, T_p	40
Number of teeth gear, T_g	127
Module, m (mm)	1.25
Pressure angle, α	20
Addendum factor, ha	1.25
Face width, b (mm)	15

TABLE II. Mechanical properties of gear materials

Parameters	Values
Density of material, kg/m^3	7800
Yield stress (MPa)	986
Poisson ratio	0.29
Modulus of elasticity (GPa)	190
Brinell Hardness	311

B. Model of a gear tooth

The section curve equation can be divided into five parts, including the downward curve, downward transition curve, upward involute curve, upward transition curve, and addendum curve.

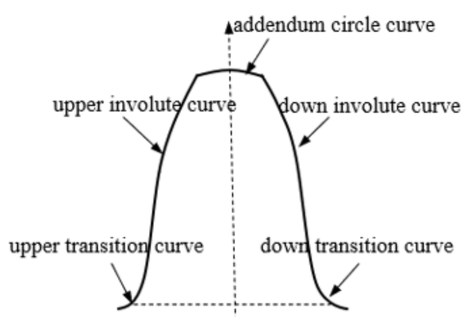

Fig 1. Basic cutter of gear tooth

The profile equation of the gear tooth is used in equation (1) to construct the new model. The section of the gear is symmetric about the x_g axis, and the center of the gear is at the coordinate point O.

$$y_{gw} = \frac{\pi m}{4} + x_g m_n \tan\alpha$$

$$x_{gc} = h_{ga} m_n - x_g m_n - \rho_f \sin\alpha$$

$$y_{gc} = y_{gw} + x_{gc}\tan\alpha + \frac{\rho_f}{\cos\alpha}$$

$$\gamma_g = \arctan\left(\frac{r_g}{x_{gc}} - \frac{y_{gc}}{x_{gc}}\right) \qquad \text{Eq: (1)}$$

$$\alpha_{gc} = \mathrm{acos}\left(\frac{r_g}{r_{ga}\cos\alpha}\right)$$

Where, y_{gw} is the half length of the cutter pitch line, m_n is the normal module, x_g is the addendum modification coefficient, x_{gc}, y_{gc} is the center locations of edge radius of cutter, r_g is the reference circle radius, h_a is the addendum coefficient, r_a is the addendum circle radius, ∅ is the independent variable for the curve, ρ_f is the edge radius of cutter, and γ_g - angle of the envelope point.

C. Load distribution ratio

The first point for the pinion tooth is contact at 'g,' while the second tooth makes contact at 'c.' This results in a sharing of the load between these two points, as illustrated in Figure 2, where the applied load shares these two gear teeth.

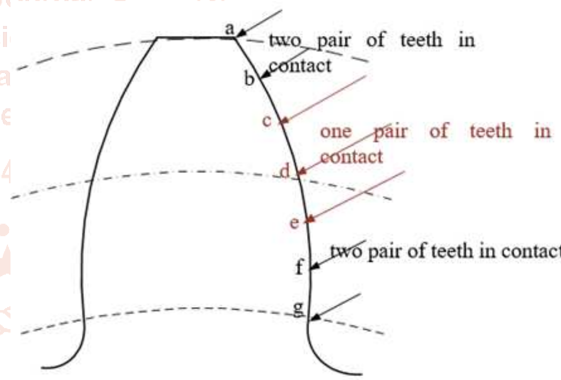

Fig 2. Gears contact position

In a similar manner, points 'f' and 'b' move simultaneously with points 'e' and 'a.' Subsequently, 'a' becomes disconnected, and the full load initially at point 'e' is transferred to point 'd' until it reaches point 'c,' where the newly connected teeth come into contact.

The gear operates with a standard contact ratio, meaning that when a single pair of teeth is engaged, that specific pair bears the entire load. However, when two pairs of teeth are in contact, the transmitted load is distributed between the teeth in the connection. This load distribution ratio depends on both the contact ratio and the stiffness of the teeth at the load point position. The load distribution ratio is particularly evident at points 'e,' 'd,' and 'C,' as shown in Figure 2.

For the cases examined, the load distribution ratios remain quite consistent, hovering around R = 0.35, and approaching R = 0.65 at the extremes of the interval where two pairs of teeth engage. At the very limit of the engagement interval for a single pair of teeth, the load-sharing ratio reaches R = 1 [15]. The load distribution ratio can be expressed as follows:

$$R(\xi)= 0.35+0.30\frac{\xi-\xi_{inn}}{\varepsilon_\alpha-1} \quad \text{for } \xi_{inn} \le \xi \le \xi_{inn}+\varepsilon_\alpha-1$$

$$(\xi)=1 \quad \text{for} \quad \xi_{inn}+\varepsilon_\alpha-1 \le \xi \le \xi_{inn}+1 \quad \text{Eq: (2)}$$

$$R(\xi)= 0.65-0.30\frac{\xi-\xi_{inn}-1}{\varepsilon_\alpha-1} \quad \text{for } \xi_{inn}+1 \le \xi \le \xi_{inn}+\varepsilon_\alpha$$

D. Taguchi Method

Table.III outlines the chosen gear parameter levels, while it shows the orthogonal arrangement of L_9. In this section, the gear profile is modified with respect to four parameters: pressure angle, addendum modification, edge radius, and face width of the gear tooth. However, the face width remains constant. Pressure angles are adjusted, and addendum modifications vary between 1.25, 1.30, and 1.38, with edge radii of fillet at 0.375 mm, 0.5 mm, and 0.625 mm.

TABLE III. Level Selection of the process parameters

Profile parameter	Level		
	1	2	3
Normal pressure angle (degree)	19	20	21
Addendum modification coefficients(mm)	1.25	1.30	1.38
Edge radius (mm)	0.375	0.50	0.625

A new method has been developed using the Taguchi method to consider four different parameter variations. The Taguchi method utilizes these four parameters as a simple, effective, and systematic approach to design optimization, encompassing performance, quality, and cost considerations. An L_9 orthogonal array with 4 columns and 9 rows is employed to facilitate the process. Initially, the Taguchi method generates nine distinct simulations, each utilizing different load distribution ratios and corresponding positions. The selection of the minimum contact position is preferred to minimize applied load[14-15]. Conversely, the maximum contact position for a single tooth pair may lead to gear failure, as noise and vibration.

Table IV. Taguchi orthogonal L_9 array for profile level selection

No	Pressure angle (degree)	Addendum modification (mm)	Edge radius (mm)
1	19	1.25	0.375
2	19	1.30	0.500
3	19	1.38	0.625
4	20	1.25	0.625
5	20	1.30	0.375
6	20	1.38	0.500
7	21	1.25	0.500
8	21	1.30	0.625
9	21	1.38	0.375

E. Analytical method of the TRS and deflection

The highest TRS occurs in the transition curve region during single tooth contact, which is in line with the gear's working principle. In single-tooth meshing, the maximum bending moment typically rises, rather than in double-tooth meshing. Furthermore, the involute curve region near the root is smaller bending moment but transition curve region is larger bending moment. The new method introduced in this paper is based on these considerations. Figure 3 shows the parameters of the TRS and deflection calculation method. Following the involute gear meshing rule, the direction of the base circle's outer tangent line at the meshing point represents the load orientation (F) on the gear. The pressure angle at the meshing point (α_{gF}) is the angle between the tangent line and the Yg axis, and it varies at different meshing positions. Additionally, ϕ_{gF} denotes the value of ϕ_{giu} at the meshing point. Taking into account the gear's stress characteristics, the standard TRS composed both standard bending moment stress and axial compressive stress.

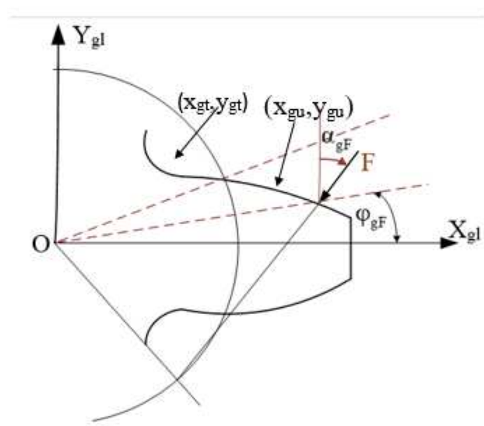

Fig 3. Parameters of analytical new model

The tangent line direction of the main circle outside the mesh point aligns with the load direction (F) on the gear. The pressure angle at the mesh point (α) equals the angle between the tangent line and the ygi axis, and it varies at different positions. Additionally, ϕg represents the value at the mesh point. The new model was chosen based on modifications to gear profile parameters, including adjustments to the pressure angle, addendum factor, and edge radius, using the Taguchi method. The pressure angle is adjusted from 19° to 21°, the addendum modification is varied from 1.0 to 1.1 times the module, and the edge radius is changed from 0.3 to 0.5 times the module. Considering the load characteristics of the gears, the standard tooth root stress comprises both standard bending moment and axial stress.

The stress due to bending moment is expressed by Equation: 3. [5]

$$\sum\sigma_g = \frac{3F\{[x_{gu}(\varphi_g)-x_{gt}(\varphi_g)]\cos\alpha_g - y_{gu}(\varphi_g)\}\times\sin\alpha_g}{2\times b\times y_{gt}^2(\varphi_g)} \quad \text{Eq:(3)}$$

Where, x_g is the addendum modification coefficient, α is the normal pressure angle, x_{gt}, y_{gt} is the center locations of edge radius of cutter.

The standard axial compressive stress can be expressed by Equation: (4).

$$\sigma_a = \frac{F\sin\alpha}{2\times b\times y(\varphi_g)} \quad \text{Eq:(4)}$$

The total standard stresses are obtained by using the Equations: (5) and (6), these equations are based on the base of gear tooth. Total standard compressive stress is achieved as follow:

$$\sigma_c = \sigma_g + \sigma_a \quad \text{Eq: (5)}$$

Total standard tensile stress:

$$\sigma_t = \sigma_g - \sigma_a \quad \text{Eq: (6)}$$

F. Deflection of gear tooth

The deflection of gear tooth is calculated by the following eq: (7).

$$\text{Deflection, } \delta = \frac{A}{B} \quad \text{Eq: (7)}$$

In this equation,

$$A = F_t \times L^3$$

$$B = 3\times E\times I$$

Where, F_t is the tangential applied load (N), L is the tooth height, E is the modulus of elasticity (N/mm^2), I is the moment of inertial of gear tooth (mm^4)

In this approach the strength is modified by various factors that produce limiting values of the bending stress.

$$S_t = (0.533H_B + 88.3)\ \text{MPa} \quad \text{Eq: (8)}$$

F. Analytical Results

The load distribution on the gear teeth is determined using Eq. (2) at nine different positions.

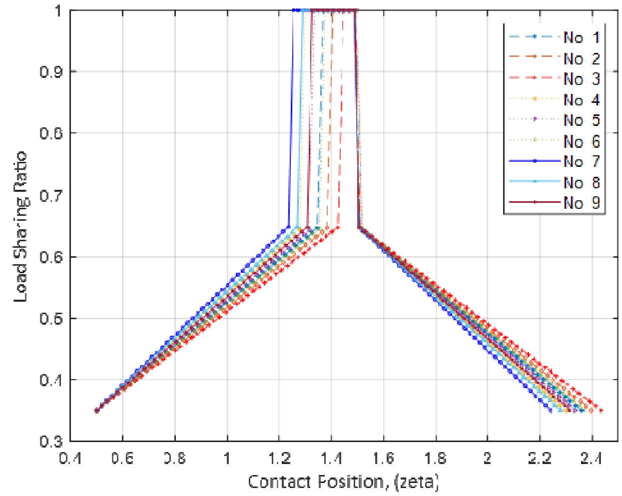

Fig 4. Load sharing ratio for all simulations

Figure 2 illustrates the location of the load distribution ratio from the bottom to the tip of the gear tooth. The relationship between the load distribution along the gear teeth is depicted in Figure 4. This paper examines the applied load from the base to the tip of the gear tooth, considering changes in the gear tooth profile facilitated by the Taguchi method. The initial contact points are the same, but the final contact point differs. Changes in the addendum factor and pressure angle result in variations in contact lengths and contact ratios. Due to these factor adjustments, the maximum load-sharing ratio position is identified at 0.24 mm in Simulation 7, represented by the blue color. Conversely, the minimum load-sharing ratio position is at 0.07 mm in Simulation 3, indicated by the red color. Comparing these two simulations, the maximum load-sharing ratio position decreases by 0.17 mm. The position of the maximum load distribution ratio slightly decreases in Simulation 3. Therefore, Simulation 3 is chosen among the others. Gear failure occurs at this position as the entire load is applied here. Hence, this position will be reduced to prevent gear surface failure.

The calculation of the maximum tooth root stress (TRS) and deflection is performed using the results obtained from the load distribution ratio in all simulations. Tables V. display the contact positions and the maximum stress due to the applied load along the tooth flank in simulations conducted with new methods.

TABLE.V. Tooth root stress (using new method) and contact position.

No	point g to point e	point e to point c	point c to point a	Tooth root stress (MPa)
1	0.80	0.14	0.80	185.84
2	0.84	0.10	0.84	185.84
3	0.88	0.07	0.88	185.84
4	0.75	0.20	0.75	185.84
5	0.78	0.16	0.78	185.84
6	0.82	0.12	0.82	185.84
7	0.69	0.24	0.69	185.84
8	0.73	0.21	0.73	185.84
9	0.76	0.18	0.76	185.84

Table V displays the contact position and maximum tooth root stress using the new method along the gear tooth. The maximum tooth root stress (185.84 MPa) occurs when all loads are applied between points 'e' and 'c.' The minimum contact position is observed in Simulation 3, making it the position with the smallest gear failure due to the applied load.

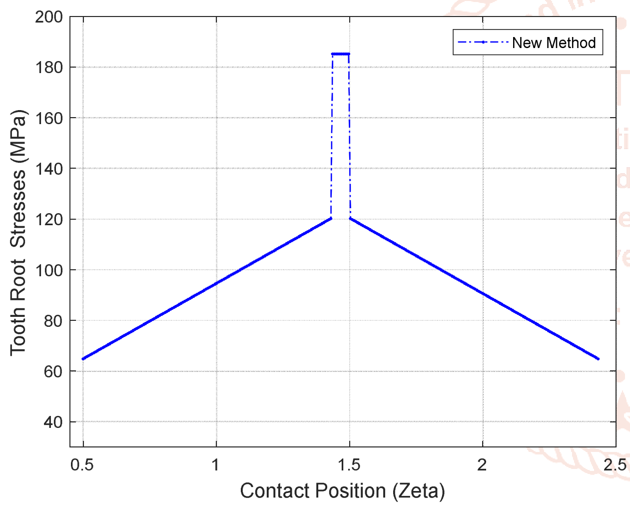

Fig 5. Maximum Tooth Root Stress (MPa)

Figure 5 illustrates the distribution of tooth root stress at various positions, ranging from the tooth root to the tip, using four different methods. The stresses exhibit a gradual increase from the contact position of 0.5 mm to 1.42 mm. The stress sharply decreases from 1.5 mm to 2.42 mm. The maximum tooth root stress is observed when the load is applied at 1.5 mm from the base of the gear tooth.Although the value of the maximum tooth root stress in the new method is nearly the same as that in the ISO method, the shape of the tooth root stress in the ISO method differs from the other methods.

G. FEM Results

The FEM method employs ANSYS software. The simulation results indicate that the quality of the mesh product is influenced by the element quantity, aspect ratio, and skewness. Typically, increasing the number of nodes (or elements) yields a more accurate result, but only up to a certain limit. Consequently, the simulation result is governed by the elements and nodes, considering the element quantity, aspect ratio, and skewness. The values for elements and nodes in the FEM method are 1244019 and 292892.

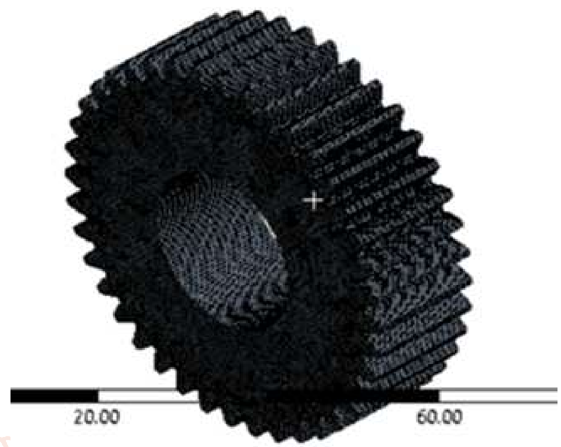

Fig 6. Use the meshing of pinion

Figure 6 displays the mesh of the pinion tooth. The element quantity for this gear is 0.85652, falling within the range of 0.7 to 0.95, indicating good quality. Subsequently, the simulation checks the aspect ratio, resulting in a value of 1.3809.

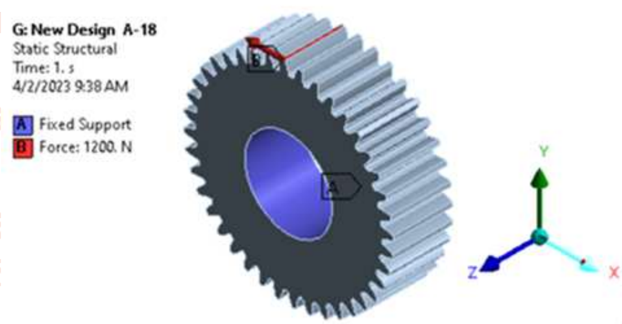

Fig 7. Boundary Condition of Pinion

An aspect ratio of less than 5 is considered good quality for most elements (90% and above). The simulation also assesses skewness, with a value of 0.19262 falling within the range of 0 to 0.25, indicating excellent quality. Skewness is a crucial criterion for mesh quality in a static structure, defining the error of cell shape and its equivalent volume. A skewness value closer to one suggests decreased accuracy.

The boundary condition is expressed as a fixed position in the center of the gear, with an applied load of 1200 N acting on the gear tooth as shown in figure 7.

Tooth root stress distribution is depicted in Figure 8, with the highest concentration observed at the base of the gear tooth.

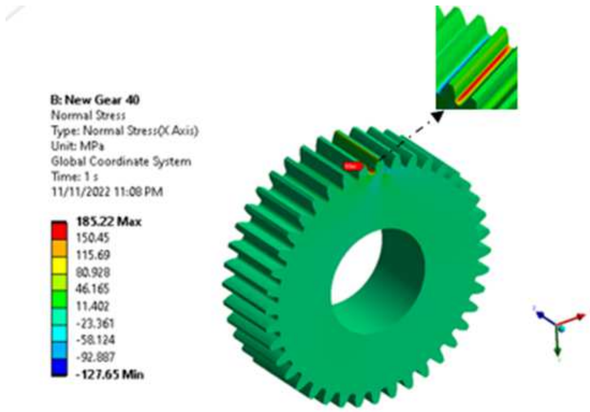

Fig 8. Tooth root stress of simulation 3

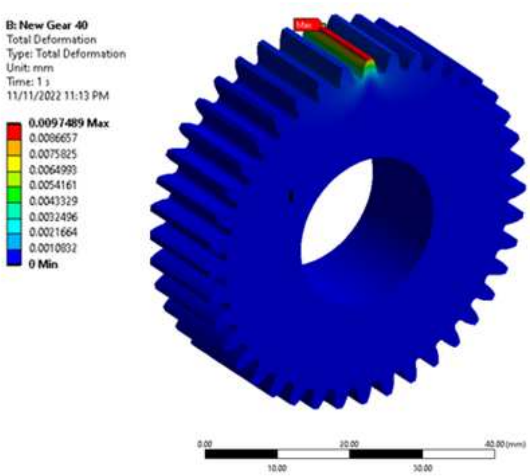

Fig 9. deflection with ANSYS software.

The maximum deflection, measuring 0.0097 mm, occurs at the tip of the gear tooth and expresses in red color line.

H. Conclusion

The deflections of the spur gear tooth are the same in all methods because the maximum applied load value is constant. The results of deflection with analytical method is 0.0110 mm and FEM method is 0.0097 mm. The error of these two method is a little different (0.0013mm).The gear used in lathe machine was analyzed by using analytical method such as new method and numerical method such as FEM method used ANSYS software. The detail results of tooth root stress values are 185.84 MPa for the new model method, and 185.22 MPa for the FEM method. The allowable strength is 254.06 MPa. So, the maximum tooth root stress of the new method is close to the FEM method. According to these two results, the difference in tooth root stress is 1%. Therefore, the tooth root stress of spur gear is sharply decreased than the allowable bending stress of the material. The analyzed of new profile spur gear will not be failure due to these tooth root stresses.

I. Discussion

First, the exact profile equation for the involute spur gear is established. Then, the maximum tooth root stress and deflection of the new method are calculated with different tooth normal pressure angles, addendum coefficients, and fillet edges, and are compared with the FEM method through numerical. Finally, the results of the new analytical methods are compared to the FEM method. The new method utilizes an analytical approach based on mechanics theory and possesses stronger theoretical properties. When calculating the maximum tooth root stress (TRS), both the axial compressive stress and the bending stress are considered in the new method.

References

[1] AGMA Standard 2001-D04, American Gear Manufactures Association, Alexandria, VA, 2004.

[2] ISO Standard 6336-1,International Organization for Standardization, Geneva, Switzerland, 2006.

[3] ISO Standard 6336-2, Calculation of Load Capacity of Spur and Helical Gears-Part 2: Calculation of Surface Durability (Pitting), International Organizattion for Standardization, Geneva, Switzerland,2006.

[4] ISO Standard 633-6, International Organization for Standardization,Geneva,Switzerland,2006.

[5] T. H. Chong. T. Suzuki. T. Aida. H. Fujio, Bending Stresses on internal Spur Gears, JSME Bull. 25(1982) 679-686.

[6] T. H. Chong. A. Kubo. Simple stress formulae for a thin-rimmed spur gear (Parts 1-3), J. Mech. Trans. Autom. Des. 107 (1985) 406-422.

[7] S. Li, Finite element analyses for contact strength and bending strength of a pair of spur gears with machining errors, assembly errors and tooth modifications, Mech. Mach. Theory 42 (2007) 88–114.

[8] M. B. Sánchez, M. Pleguezuelos, J.I. Pedrera, Tooth-root stress calculation of high transverse contact ratio spur and helical gears, Meccanica 49 (2014) 347–364.

[9] J. Wang, I. Howard, Finite element analysis of high contact ratio spur gears in mesh, J. Tribol. 127 (2005) 469–483.

[10] P. Marimuthu, G. Muthu Veerappan, Optimization of fillet stress to enhance the bending strength through non-standard high contact ratio spur gears, in: Proceedings of the Institution of Mechanical Engineers, Part C: Journal of Mechanical Engineering Science, 230, 2016, pp. 1139–1148

[11] V. S. Kumar, D.V. Muni, G. Muthuverapan, Optimization of asymmetric spur gear drives to improve the bending load capacity, Mech. Mach. Theory 43 (2008) 829–858.

[12] N.L. Pedersen, improving bending stress in spur gears using asymmetric gears and shape optimization, Mech. Mach. Theory 45 (2010) 1707–1720.

[13] I. Gonzalez-Perez, A. Fuentes-Aznar, Implementation of a finite element model for stress analysis of gear drives based on multi-point constraints, Mech. Mach. Theory 117 (2017) 35–47.

[14] M. J. Wang, A new photo-elastic investigation of the dynamic bending stress of spur gears, J. Mech. Des. 125 (2003) 365–372

[15] V. A. Spitas, Optimum gear tooth geometry for minimum fillet stress using BEM and experimental verification with photoelasticity, Drive Syst. Tech. 128 (2007) 1159–1164.